PRAMANA
— journal of
physics

Vol. 75, No. 1
July 2010
pp. 39–49

Ab-initio Hamiltonian approach to light nuclei and to quantum field theory

J P VARY[1,*], H HONKANEN[1], JUN LI[1], P MARIS[1], A M SHIROKOV[2], S J BRODSKY[3], A HARINDRANATH[4], G F DE TERAMOND[5], E G NG[6], C YANG[6] and M SOSONKINA[7]

[1]Department of Physics and Astronomy, Iowa State University, Ames, Iowa 50011, USA
[2]Skobeltsyn Institute of Nuclear Physics, Moscow State University, Moscow 119992, Russia
[3]SLAC National Accelerator Laboratory, Stanford University, Stanford, California 94309, USA
[4]Theory Group, Saha Institute of Nuclear Physics, 1/AF, Bidhan Nagar, Kolkata 700 064, India
[5]Universidad de Costa Rica, San José, Costa Rica
[6]Lawrence Berkeley National Laboratory, Berkeley, California, USA
[7]Ames Laboratory, Iowa State University, Ames, Iowa 50011, USA
[*]Corresponding author. E-mail: jvary@iastate.edu

Abstract. Nuclear structure physics is on the threshold of confronting several long-standing problems such as the origin of shell structure from basic nucleon–nucleon and three-nucleon interactions. At the same time those interactions are being developed with increasing contact to QCD, the underlying theory of the strong interactions, using effective field theory. The motivation is clear – QCD offers the promise of great predictive power spanning phenomena on multiple scales from quarks and gluons to nuclear structure. However, new tools that involve non-perturbative methods are required to build bridges from one scale to the next. We present an overview of recent theoretical and computational progress with a Hamiltonian approach to build these bridges and provide illustrative results for the nuclear structure of light nuclei and quantum field theory.

Keywords. Microscopic nuclear structure; no core shell model; light-front field theory.

PACS Nos 21.10.-k; 21.60.De; 11.15.Tk; 12.20.-m; 12.38.-t

1. Introduction

Recent advances in achieving *ab-initio* solutions of the non-relativistic quantum many-body problem, with strong interactions based on quantum chromodynamics (QCD), have raised the promise that the properties of atomic nuclei may be derived from first principles. Along with this comes the prospect that a microscopic approach with meaningful predictive power is emerging. The capability to predict reactions not accessible in laboratory experiments, along with quantified uncertainties, has major implications for nuclear astrophysics and for applications

to nuclear energy and other fields. Furthermore, achieving accurate nuclear wave functions signals the advent of precision tests of fundamental symmetries and access to physics beyond the Standard Model. Neutrinoless double beta decay is a leading example where precision nuclear matrix elements would play a major role in the interpretation of the experiments that are underway or are in the planning phases.

A successful microscopic non-perturbative Hamiltonian approach to low-energy nuclear physics also has major implications for the eventual direct solution of QCD in the framework of light-front quantization. Beyond achieving a successful description of hadron spectroscopy, light-front Hamiltonian field theory promises to produce the amplitudes that would generate, among other experimental quantities, the celebrated generalized parton distribution functions. At the fundamental level, these amplitudes would reveal the spin content of the proton and resolve the current experimental puzzle, sometimes referred to as the 'spin crisis'.

In this paper, we review some highlights of the recent progress that illuminate the path we are pursuing. We illustrate key ingredients of the theoretical frameworks and the role of leadership class computers.

2. Hamiltonian many-body theory

Non-relativistic quantum mechanics for many particles lies at the heart of our approach. We will indicate that this approach, with suitable changes, is sufficient for a covariant treatment of relativistic quantum field theory. We adopt the quantum Hamiltonian matrix formulation of the eigenvalue problem in the Dirac notation for the Hermitian many-body Hamiltonian H:

$$H|\Psi_i\rangle = E_i|\Psi_i\rangle. \tag{1}$$

We also expand the eigenvectors $|\Psi_i\rangle$ in a set of convenient basis states $|\Phi_j\rangle$:

$$|\Psi_i\rangle = \sum_j A_{ij}|\Phi_j\rangle. \tag{2}$$

The overall task is then to evaluate the chosen Hamiltonian in the selected finite basis space and carry out the diagonalization to produce the eigenvalues E_i and the eigenvectors $|\Psi_i\rangle$ at least for the low-lying spectra. Convergence is measured by increasing the size of the finite basis until the low-lying spectra become independent of parameters defining the basis space and independent of the cut-off. One employs the resulting eigenvectors to evaluate matrix elements of observables that are compared with experiment where available.

Our approach is simple, direct and intuitive. However, there are major theoretical and computational challenges. The path forward can be represented by the answers to a set of key questions:

1. What are the interactions defining the Hamiltonian?
2. What is the physically sensible basis space?
3. How to preserve all the symmetries imbedded in H?
4. How to renormalize the Hamiltonian for the chosen finite basis space?

5. How to numerically solve the large sparse matrix eigenvalue problem?
6. How is convergence measured and how are uncertainties assessed?

While space does not permit detailed answers here, we will introduce some of the key elements with references to the literature. One point that deserves special mention is the great technical progress that has been achieved in solving the large sparse matrix eigenvalue problem with the Lanczos algorithm on leadership class computers [1–3].

3. Applications to light nuclei

Specific answers to these questions have been developed for the *ab-initio* no core shell model (NCSM) [4] and no core full configuration (NCFC) [5] approaches to solve nuclear structure with realistic nucleon–nucleon (NN) and three-nucleon (NNN) interactions.

In the realization of the NCSM with close ties to QCD, one adopts a finite basis-space renormalization method and applies it to realistic nucleon–nucleon (NN) and three-nucleon (NNN) interactions (derived from chiral effective field theory) to solve nuclei with atomic numbers $A = 10$–13 [6]. Experimental binding energies, spectra, electromagnetic moments and transition rates are well-reproduced.

In the NCFC approach [5], one adopts a realistic NN interaction that is soft enough that renormalization may not be necessary and binding energies obtained from a sequence of finite matrix solutions may be extrapolated to the infinite matrix limit. Owing to the variational principle and uniform convergence, one is able to assess the theoretical uncertainties in the extrapolated result. One again obtains good agreement with experiment.

The primary advantages of these methods are the flexibility for choosing the Hamiltonian, the method of renormalization/regularization and the basis space. These advantages impel us to adopt the basis function approach in light-front quantum field theory which we discuss further below.

In our applications to light nuclei we select the 3D harmonic oscillator for the single fermion states and construct the many-body basis states by enumerating all unique, Pauli-allowed, states with the total number of oscillator quanta limited by $N_{\max}$, the number of oscillator quanta above the minimum needed for the nucleus under consideration. Thus $N_{\max}$ and the harmonic oscillator energy $\hbar\Omega$ represent the two parameters characterizing the finite basis representation of the eigenstates. Results independent of these two basis space parameters are considered to be the converged exact results for that Hamiltonian.

We present in figure 1 the spectra of ^{6}Li in the NCFC approach with the realistic JISP16 NN interaction [7]. The progression of the eigenenergies from the left-most column, proceeds with increasing $N_{\max}$ towards convergence and are connected by solid lines. The experimental results are given in the right-most column. Two methods of extrapolation are presented, referred to as 'A' and 'B', along with their assessed uncertainties. Results for 'B' are connected by dotted lines while results for 'A' are presented in the column close to the experimental results. The agreement in total energies is good and the level ordering is correct. There is an overall shift of about 0.4 MeV between the converged results and experiment. The RMS deviation

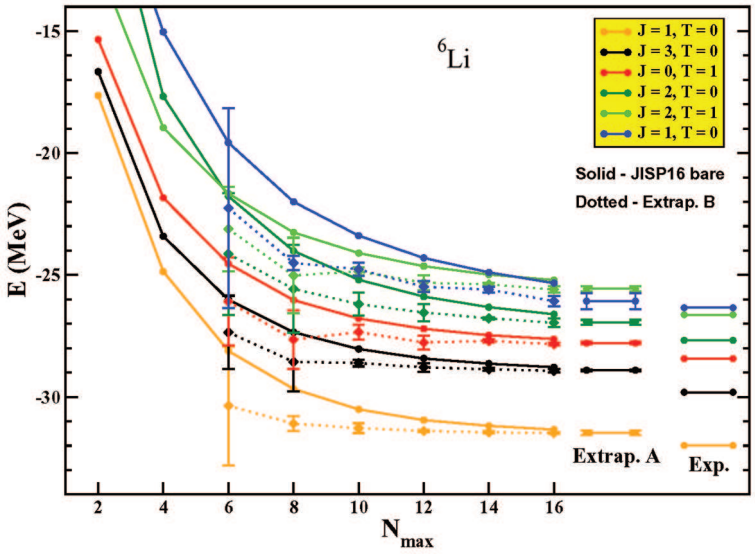

Figure 1. Spectra of ^{6}Li obtained in a sequence of basis space truncations up to $N_{\max} = 16$ and extrapolated with two different methods, 'A' and 'B', described in ref. [5] and compared with experiment.

between theory and experiment is 0.739 MeV for the total energies. The RMS deviation in excitation energies above the ground state is 0.336 MeV. The residual differences may be ascribed to the neglect of a three-body force.

It is important to note that the Gamow–Teller matrix element for β-decay from ^{6}He to ^{6}Li has been investigated in detail [8] with the same JISP16 interaction and found to be within 2% of the experimental result. It was previously reported that the ground state quadrupole moment of ^{6}Li, which involves large cancellations, is close to the experimental results with JISP16 [7]. The overall impression is that we have achieved an excellent description of the low-lying properties of ^{6}Li.

Figure 2 provides another view of the present status of *ab-initio* microscopic nuclear many-body theory with the eigenenergies of the first excited 0^+ of ^{12}C as a function of the oscillator energy $\hbar\Omega$ for values of $N_{\max}$ incrementing by 2 from 2 through 8. In addition, we include two recently calculated points at $N_{\max} = 10$. The latter two points represent solving for the low-lying eigenvalues of a matrix with dimension 7,830,355,795. Each of these solutions required 8 h of wall-clock time on approximately 100,000 cpu's of the Jaguar Facility at Oak Ridge National Laboratory. With a few additional $N_{\max} = 10$ points, we will be able to update the extrapolation shown in the figure and reduce the uncertainty by an estimated factor of 2.

4. Approach to quantum field theory

Hamiltonian light-front quantum field theory has a long history [9]. Our approach is to establish a convenient basis space expansion of the light-front amplitudes by

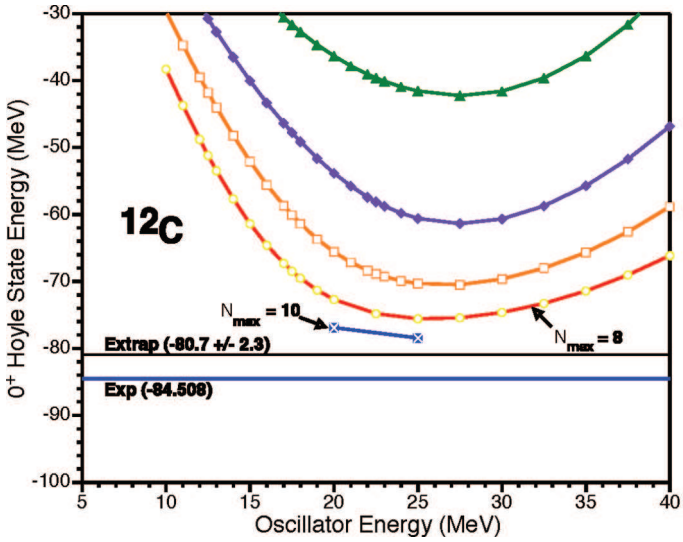

Figure 2. Energy of the first excited 0^+ state in ^{12}C as a function of oscillator energy $\hbar\Omega$ for values of $N_{\max}$ incrementing by 2. The extrapolated result indicated in the figure is based on method 'A' of ref. [5] and employs only the results through $N_{\max} = 8$.

solving the sparse Hamiltonian matrix eigenvalue problem following the techniques developed for the *ab-initio* no core methods outlined above. We refer to our approach as the basis light-front quantization (BLFQ) method. Recently, we have presented our initial applications of this method [10,11] and we summarize here the main ingredients.

We define the radial coordinate ρ and polar angle ϕ, the usual cylindrical coordinates in (x^1, x^2), $x^{\pm} = x^0 \pm x^3$ and $x^{\perp} = (x^1, x^2)$ for our light-front coordinates. The variable x^+ is taken to be the light-front time and x^- is the longitudinal coordinate. We take the 'null plane', $x^+ = 0$, for our quantization surface. In the BLFQ approach we adopt a light-front single-particle basis space consisting of the 2D harmonic oscillator for the transverse modes in (ρ, ϕ) and a discretized momentum space basis for the longitudinal modes. Note that this basis is consistent with recent developments in AdS/CFT correspondence with QCD [12–16]. We omit the longitudinal zero mode when choosing periodic boundary conditions and note that they are absent when choosing antiperiodic boundary conditions.

The 2D oscillator states are characterized by their principal quantum number n, orbital quantum number m and harmonic oscillator energy Ω. It is convenient to interpret the 2D oscillator as a function of the dimensionless radial variable $\sqrt{M_0\Omega}\rho$ where M_0 has units of mass and ρ is in units of length. Thus, the length scale for transverse modes is set by the chosen value of $\sqrt{M_0\Omega}$.

The properly orthonormalized wave functions, $\Phi_{n,m}(\rho, \phi) = \langle \rho\phi | nm \rangle = f_{n,m}(\rho)\chi_m(\phi)$, are given in terms of the generalized Laguerre polynomials, $L_n^{|m|}(M_0\Omega\rho^2)$, by

$$f_{n,m}(\rho) = \sqrt{2M_0\Omega}\sqrt{\frac{n!}{(n+|m|)!}}\mathrm{e}^{-M_0\Omega\rho^2/2} \times \left(\sqrt{M_0\Omega}\rho\right)^{|m|} L_n^{|m|}(M_0\Omega\rho^2) \quad (3)$$

$$\chi_m(\phi) = \frac{1}{\sqrt{2\pi}}\,\mathrm{e}^{im\phi} \quad (4)$$

with 2D harmonic oscillator eigenvalues $E_{n,m} = (2n + |m| + 1)\Omega$. The orthonormalization is fixed by

$$\langle nm|n'm'\rangle = \int_0^\infty \int_0^{2\pi} \rho\,\mathrm{d}\rho\;\mathrm{d}\phi\Phi_{n,m}(\rho,\phi)^*\;\Phi_{n',m'}(\rho,\phi) = \delta_{n,n'}\delta_{m,m'} \quad (5)$$

which allows for an arbitrary phase factor $\mathrm{e}^{i\alpha}$ that we have taken to be unity. The Fourier transformed wave functions, the momentum space wave functions, have the same analytic structure in both coordinate and momentum space, a convenient feature reminiscent of a plane-wave basis.

In an initial application of the BLFQ approach, we consider an electron confined to a transverse harmonic trap or cavity. Our goal is to evaluate the anomalous magnetic moment, the anomalous gravitomagnetic moment, and various form factors of the electron arising from QED. We evaluate these observables and take the limit where the cavity is removed to compare with results from perturbation theory.

We implement a transverse 2D harmonic oscillator basis with length scale fixed by the trap and finite modes in the longitudinal direction with antiperiodic (periodic) boundary conditions for the fermions (bosons). We plan to adopt the NCSM method for factorizing the eigensolutions into simple products of intrinsic and total momentum solutions in the transverse direction [4]. Following ref. [9] we introduce the total invariant mass-squared M^2 for these low-lying physical states in terms of a Hamiltonian H times a dimensionless integer for the total light-front momentum K

$$M^2 + P_\perp P_\perp \to M^2 + \text{const.} = P^+P^- = KH, \quad (6)$$

where we absorb the constant into M^2. The Hamiltonian H for this system is defined to include an unperturbed cavity contribution, a sum of the occupied modes i in each many-parton state that involves a scale set by the combined constant $\Lambda^2 = 2M_0\Omega$:

$$H = 2M_0P_c^- = \frac{2M_0\Omega}{K}\sum_i \frac{2n_i + |m_i| + 1}{x_i} + H_I. \quad (7)$$

In eq. (7) the term H_I represents lepton–photon vertices arising from QED. Within the light-front treatment there are only two classes of such vertices. In the first class, we have a lepton emitting or absorbing a photon plus other time orderings where, for example, a photon transforms to a lepton–antilepton pair. In the second class we have an instantaneous interaction between a lepton and a photon, higher-order terms that arise from a constraint equation.

We adopt symmetry constraints corresponding to properties of QED and two cut-offs for our many-parton states. For symmetries, we fix the total charge Z and the total angular momentum projection quantum number M_j along the x^- direction. For cut-offs, we select the total light-front momentum, K, and the maximum total quanta allowed in the transverse mode of each many-parton state, $N_{\max}$. The chosen symmetries and cut-offs are expressed in terms of sums over the quantum numbers of the single-parton degrees of freedom contained in each many-parton state of the system in the following way:

$$\sum_i q_i = Z, \tag{8}$$

$$\sum_i m_i + s_i = M_j, \tag{9}$$

$$\sum_i x_i = 1 = \frac{1}{K}\sum_i k_i, \tag{10}$$

$$\sum_i 2n_i + |m_i| + 1 \leq N_{\max}, \tag{11}$$

where k_i is the half integer (integer) that defines the longitudinal modes for the ith fermion (boson). The range of the number of fermion–antifermion pairs and bosons is limited by the cut-offs in the modes (K and $N_{\max}$) since each parton carries a finite amount of longitudinal momentum. Furthermore, since each parton carries at least one oscillator quanta for transverse motion, the basis is also limited to $N_{\max}$ partons. One may also elect to truncate the many-parton basis by limiting the number of fermion–antifermion pairs and/or the number of bosons. For our initial application here, where we intend to compare with results from low-order perturbation theory, we limit the basis to single lepton and lepton–photon basis states.

Since we work in a transverse 2D oscillator basis and assign a transverse motion single-particle state for each parton, the basis is complete in that it specifies the motion of the system's centre of mass (CM). The special properties of the harmonic oscillator allow the factorization of each solution into an amplitude of intrinsic motions times the amplitude of the CM motion with the method of regularization we have chosen. We can then easily divide out that CM motion component as the need arises in subsequent calculations that employ the resulting amplitudes.

In figure 3 we show the eigenvalues (multiplied by K) for a light-front QED Hamiltonian in a basis space limited to the fermion and fermion–boson sectors. For this particular example we chose the harmonic oscillator parameters as $\Omega = 0.1$ MeV and $M_0 = 0.511$ MeV, and the fermion mass was chosen to be equal to M_0. We chose the basis space such that the basis states have total $M_j = M_t + S = \frac{1}{2}$, and we simultaneously increase the K and $N_{\max}$ cut-offs. As a result, the sizes of the Hamiltonian matrices increase rapidly. For $K = N_{\max} = 2, 3, 4, 5$, the dimensions of the corresponding matrices are 2×2, 12×12, 38×38 and 99×99 respectively.

The number of the single fermion basis states increases slowly with increasing $K = N_{\max}$ cut-off. For $K = N_{\max} = 2, 3, 4, 5$ the number of single fermion basis states is $1, 2, 2, 3$, respectively. Our lowest-lying eigenvalues correspond to solutions

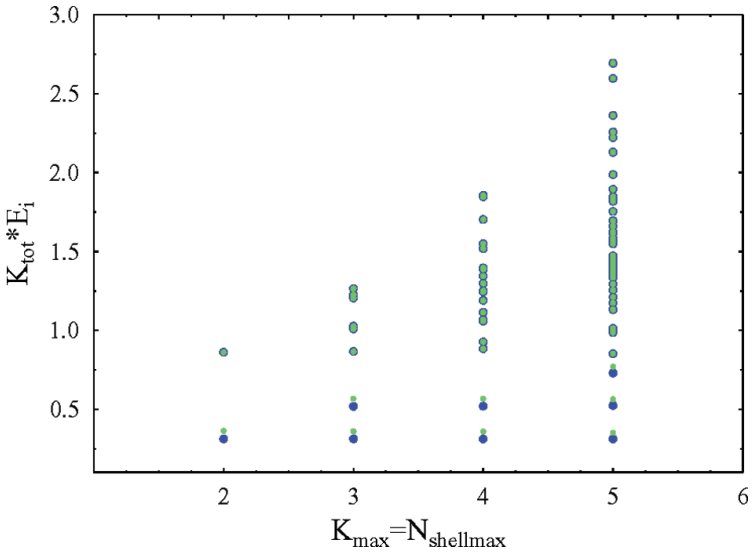

Figure 3. Mass eigenstates of a single electron in a transverse cavity as a function of the cut-offs up through $K = N_{\max} = 5$. The light (dark) dots signify the eigenvalues before (after) renormalization to the physical electron mass.

dominated by these states and they appear with nearly harmonic separations in figure 3 as would be expected at the coupling of QED.

The higher eigenstates are the ones dominated by the fermion–boson basis states that interact with each other in leading order through the instantaneous fermion–boson interaction. Their multiplicity increases rapidly with increasing $K = N_{\max}$ and they exhibit significant mixing with each other as well as weak mixing with the lowest-lying states. The eigenvalues dominated by the fermion–boson basis states cluster in nearly degenerate groups above the lowest-lying states.

Note that there are two spectra presented at each value of $K = N_{\max}$ in figure 3 signified by the lighter and the darker dots. The lighter dots represent the results of straightforward diagonalization of eq. (7) in that light-front basis. The darker dots represent the results after a renomalization process to fix the lowest mass eigenvalue at the physical mass of the electron. We adopt the renormalization procedure termed 'sector-dependent renormalization' [17], which, for the weak coupling of QED and the cavity used here, represents small adjustments in the mass eigenstates as seen in figure 3.

5. Progress towards QCD

We can extend the BLFQ approach to solve for mesons and baryons within QCD by implementing the $SU(3)$ colour degree of freedom for each parton – three colours for each fermion and eight for each boson. We consider two versions of implementing the global colour-singlet constraint for this restricted situation. In both cases

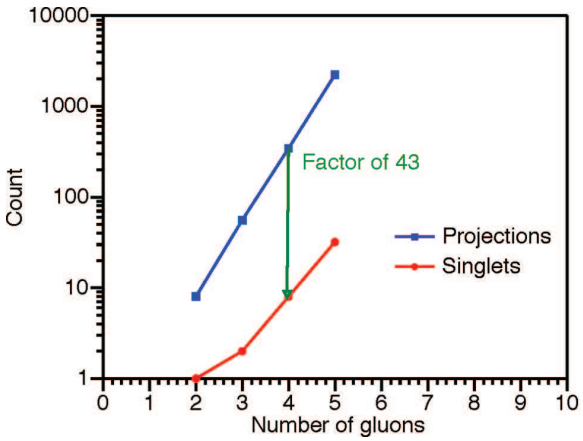

Figure 4. Number of colour space states that apply to each space-spin configuration of multi-gluon states for two methods of enumerating the colour basis states. The upper curves are counts of all colour configurations with zero colour projection. The lower curves are counts of the global colour singlets alone.

we enumerate the colour space states to integrate with each space-spin state of the corresponding partonic character. For simplicity, we will restrict the present illustration to the case of multi-gluon states.

In the first case, we follow ref. [18] by enumerating the single parton states with all possible values of $SU(3)$ colour. Thus each space-spin fermion state goes over to three space-spin colour states. Similarly, each space-spin boson state generates a multiplicity of eight states when $SU(3)$ colour is included. We then construct all many-parton states having zero colour projection. Within this basis one will have all the allowed global colour-singlet states along with some of the allowed colour non-singlet states. Within a dynamical calculation, the global colour-singlet states are isolated by adding a Lagrange multiplier term in many-parton colour space to the Hamiltonian so that the unphysical colour non-singlet states are pushed higher in the spectrum away from the physical colour single states. To evaluate the multiplicative factor governing the increase in basis space dimension arising from this treatment of colour, we enumerate the resulting colour-singlet projected colour space states for multi-gluon basis states and display the results as the upper curves in figure 4.

In the second case, we restrict the basis space to global colour singlets and this results in the lower curves in figure 4. The second method, presented in ref. [19], produces a typical factor of 30–40 lower multiplicity at the upper ends of these curves at the cost of increased computation time for matrix elements of the interacting Hamiltonian. That is, each interacting matrix element of QCD in the global colour-singlet basis is a transformation of a submatrix in the zero colour projection basis. Either implementation of colour dramatically increases the state density over the case of QED, but the use of a global colour-singlet constraint is clearly more effective in minimizing the dramatic increase in basis space states due to the colour degree of freedom.

We note that, for the pure multi-fermion basis space sector we could also use the methods introduced and applied successfully in 1+1-dimensional QCD [20]. That is, the number of global colour singlets for a given fermion-only basis state, with other (non-colour) quantum numbers specified, is independent of the number of spatial dimensions.

6. Conclusions and outlook

We have entered an era where non-perturbative solutions for quantum many-body systems within a Hamiltonian framework offers the opportunity to build a bridge from quantum field theory to the properties of atomic nuclei. When this is successful, we will have a theoretical framework with unprecedented predictive power that spans multiple physical scales. Ultimately, this offers a framework for tests of the fundamental laws of nature, such as lepton number conservation via neutrinoless double beta decay. Though we have defined a path for achieving these goals, a great deal of work is needed to achieve it. Advances in algorithm development and computational facilities will continue to play a critical role in these developments.

Acknowledgements

This work was supported by the US DOE Grants DE-FC02-09ER41582 and DE-FG02-87ER40371, FAO Contract P521 and by US DOE contract DE-AC02-76SF00515. Computational resources were provided by DOE through the National Energy Research Supercomputer Center (NERSC) and through an INCITE award (David Dean, PI); the ^{6}Li runs where performed on the Franklin supercomputer at NERSC and the ^{12}C and ^{14}B runs on Jaguar at ORNL.

References

[1] P Sternberg, E G Ng, C Yang, P Maris, J P Vary, M Sosonkina and H V Le, in: *Proceedings of the 2008 ACM/IEEE Conference on Supercomputing* (Austin, Texas, November 15–21, 2008); *Conference on High Performance Networking and Computing* (IEEE Press, Piscataway, NJ) 1-12, doi= http://doi.acm.org/10.1145/1413370.1413386.

[2] M Sosonkina, A Sharda, A Negoita and J P Vary, *Lecture notes in computer science* edited by M Bubak, G D V Albada, J Dongarra and P M A Sloot, Vol. 5101, pp. 833–842 (2008)

[3] J P Vary, P Maris, E Ng, C Yang and M Sosonkina, *J. Phys.: Conf. Ser.* **180**, 12083 (2009) doi:10.1088/1742-6596/180/1/012083; arXiv:nucl-th 0907.0209

[4] P Navrátil, J P Vary and B R Barrett, *Phys. Rev. Lett.* **84**, 5728 (2000); *Phys. Rev.* **C62**, 054311 (2000)

[5] P Maris, J P Vary and A M Shirokov, *Phys. Rev.* **C79**, 014308 (2009), nucl-th/0808.3420

[6] P Navrátil, V G Gueorguiev, J P Vary, W E Ormand and A Nogga, *Phys. Rev. Lett.* **99**, 042501 (2007), nucl-th/0701038

[7] A M Shirokov, J P Vary, A I Mazur and T A Weber, *Phys. Lett.* **B644**, 33 (2007), nucl-th/0512105
[8] S Vaintraub, N Barnea and D Gazit, *Phys. Rev.* **C79**, (2009) 065501, arXiv:0903.1048
[9] For a review, see S J Brodsky, H C Pauli and S S Pinsky, *Phys. Rep.* **301**, 299 (1998)
[10] J P Vary, P Maris, A M Shirokov, H Honkanen, J Li, S J Brodsky, A Harindranath and G F de Teramond, *10th Conference on the Intersections of Particle and Nuclear Physics* edited by Marvin L Marshak, *AIP Conf. Proc.* **1182**, 917 (2009)
[11] J P Vary, H Honkanen, J Li, P Maris, S J Brodsky, A Harindranath, G F de Teramond, P Sternberg, E G Ng and C Yang, *Phys. Rev.* **C81**, 035205 (2010), arXiv:0905.1411
[12] A Karch, E Katz, D T Son and M A Stephanov, *Phys. Rev.* **D74**, 015005 (2006)
[13] J Erlich, E Katz, D T Son and M A Stephanov, *Phys. Rev. Lett.* **95**, 261602 (2005)
[14] G F de Teramond and S J Brodsky, *Phys. Rev. Lett.* **102**, 081601 (2009)
[15] S J Brodsky and G F de Teramond, *Phys. Lett.* **B582**, 211 (2004)
[16] J Polchinski and M J Strassler, *Phys. Rev. Lett.* **88**, 031601 (2002)
[17] V A Karmanov, J-F Mathiot and A V Smirnov, *Phys. Rev.* **D77**, 085028 (2008)
[18] R J Lloyd and J P Vary, *Phys. Rev.* **D70**, 014009 (2004)
[19] Jun Li, *Light front Hamiltonian and its application in QCD*, Ph.D. Thesis (Iowa State University, 2009) (unpublished)
[20] K Hornbostel, S J Brodsky and H C Pauli, *Phys. Rev.* **D41**, 3814 (1990)